

# Grain Boundary Wetting by a Second Solid Phase in Ti-Fe Alloys

*A.S. Gornakova, B.B. Straumal, A.N. Nekrasov, A. Kilmametov, and N.S. Afonikova*

The microstructure of Ti-Fe polycrystals has been studied between 595 and 815 °C in the concentration interval between 1 and 9 wt.% Fe. In these conditions, two phases, namely hexagonal  $\alpha(\text{Ti, Fe})$  and cubic  $\beta(\text{Ti, Fe})$ , are in equilibrium. The  $\alpha(\text{Ti, Fe})$  phase forms either continuous or discontinuous layers in the  $\beta(\text{Ti, Fe})/\beta(\text{Ti, Fe})$  grain boundaries (GBs). Continuous layers correspond to the complete wetting of  $\beta(\text{Ti, Fe})/\beta(\text{Ti, Fe})$  GBs by a second solid phase  $\alpha(\text{Ti, Fe})$ . Discontinuous layers correspond to the incomplete (or partial) GB wetting by a second solid phase. The temperature dependences of the portion of completely wetted GBs as well as that of the thickness of continuous GB layer of  $\alpha(\text{Ti, Fe})$  phase have been measured. Both values monotonously increase with increasing temperature.

**Keywords** grain boundaries, phase transitions, titanium alloys, wetting

## 1. Introduction

Titanium and its alloys are widely used in engineering due to their high mechanical strength, which remains present at high temperatures, corrosion resistance, heat resistance, specific strength, low density, and other useful properties (Ref 1). The high cost of titanium and its alloys are often offset by their greater work capacity, and in some cases, they are the only material from which one is able to produce equipment or construction that can operate in harsh conditions. Microstructure of titanium alloys formed by hot deformation does not undergo significant changes during the heat treatment. Iron is one of the strongest  $\beta$ -stabilizers for titanium alloys. The solubility of iron in the  $\alpha$ -titanium at room temperature is very low; at the eutectoid temperature, it does not exceed 0.5% (Ref 2). Due to a strong hardening effect, iron is used in some

titanium alloys as an alloying additive in amounts of 0.5–1.5 wt.% in structural high strength alloys, high corrosion-resistant, and high-temperature alloys. Mechanical and other performance properties of titanium alloys strongly depend on the structure and morphology of the constituent phases (Ref 3–6). The morphology of the phases in titanium alloys can be determined not only by the well-known bulk phase transitions, but also by the so-called grain boundary phase transitions (Ref 6, 7). The authors of this work recently discovered a fundamentally new phenomenon, namely the grain boundary wetting phase transitions by a second solid phase (Ref 8–11). It consists in the fact that in two-phase regions of the phase diagrams a second solid phase can be located along the grain boundaries (GBs) of the solid matrix phase either in the form of continuous layers or as a chain of lens-like particles. The morphology of the second phase is determined by the energy of GBs and interphase boundaries (IBs) and can depend on the temperature and the pressure or the concentration of the alloying elements. The goal of this work is the investigation of grain boundary wetting phase transitions by a second solid phase in the Ti-Fe alloys.

## 2. Experimental

The Ti-1 wt.% Fe, Ti-2.8 wt.% Fe, Ti-4.3 wt.% Fe, Ti-6.5 wt.% Fe and Ti-9 wt.% Fe alloys were prepared by the induction melting in vacuum from 3N5 Ti and 4N5 Fe. The 10-mm dia as-cast rods were cut into 5-mm-thick slices. Then, the polycrystalline samples were sealed in quartz ampoules (residual pressure  $P = 4 \cdot 10^{-4}$  Pa) and annealed in a two-phase region ( $\alpha\text{Ti}$ ) + ( $\beta\text{Ti, Fe}$ ) of the Ti-Fe equilibrium phase diagram (Fig. 1) (Ref 2). Annealing of the alloys has been performed in the temperature range from 595 to 815 °C, and the duration of the annealing was on average 720 h. In other words, all annealing temperatures were below the transus line [ $(\alpha\text{Ti}) + (\beta\text{Ti, Fe})$ ]/( $\beta\text{Ti, Fe}$ ) of the Ti-Fe equilibrium phase diagram (Fig. 1). After quenching in water, the samples were polished and then chemically etched. The microstructure of polycrystalline samples was investigated by the light microscopy (LM), scanning electron microscopy (SEM), and x-ray diffraction

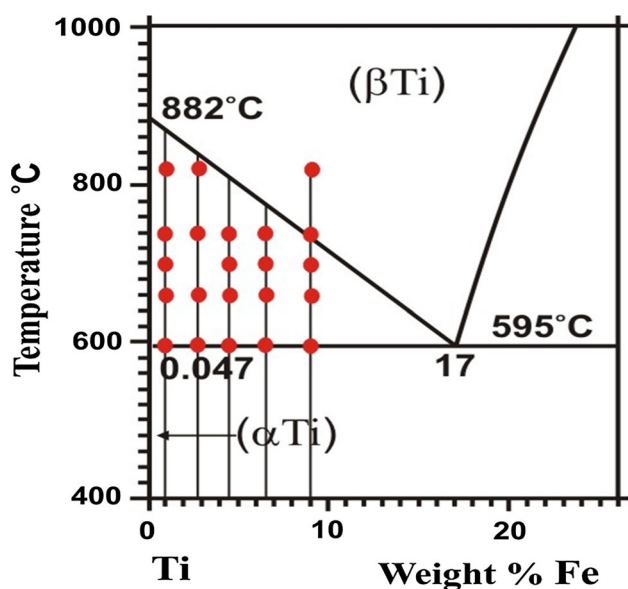
This article is an invited submission to JMEP selected from presentations at the Symposium “Interface Design and Modelling, Wetting and High-Temperature Capillarity,” belonging to the topic “Processing” at the European Congress and Exhibition on Advanced Materials and Processes (EUROMAT 2017), held September 17–22, 2017, in Thessaloniki, Greece, and has been expanded from the original presentation.

**A.S. Gornakova** and **N.S. Afonikova**, Institute of Solid State Physics, Russian Academy of Sciences, Ac. Ossipyan Str. 2, Chernogolovka, Russia 142432; **B.B. Straumal**, Institute of Solid State Physics, Russian Academy of Sciences, Ac. Ossipyan Str. 2, Chernogolovka, Russia 142432; Institut für Nanotechnologie, Karlsruher Institut für Technologie, Hermann-von-Helmholtz-Platz 1, 76344 Eggenstein-Leopoldshafen, Germany; and National University of Science and Technology «MISIS», Leninsky Pros. 4, Moscow, Russia 119991; **A.N. Nekrasov**, Institute of Experimental Mineralogy, Russian Academy of Sciences, Ac. Ossipyan Str. 4, Chernogolovka, Russia 142432; and **A. Kilmametov**, Institut für Nanotechnologie, Karlsruher Institut für Technologie, Hermann-von-Helmholtz-Platz 1, 76344 Eggenstein-Leopoldshafen, Germany. Contact e-mail: [straumal@issp.ac.ru](mailto:straumal@issp.ac.ru).

(XRD). LM has been performed using a Neophot-32 light microscope equipped with a 10 Mpix Canon Digital Rebel XT camera. SEM investigations have been carried out in a Tescan Vega TS5130 MM microscope equipped with the LINK energy-dispersive spectrometer produced by Oxford Instruments. XRD data were obtained on a Siemens D-500 diffractometer (Co K $\alpha$  radiation). A quantitative analysis of GB wetting was performed adopting the following criterion. Every  $\beta(\text{Ti, Fe})/\beta(\text{Ti, Fe})$  GB was considered to be completely wetted only when a layer of  $\alpha(\text{Ti, Fe})$  phase had covered the whole GB. If such a layer appeared to be interrupted, the GB was regarded as incompletely wetted. Boundaries with no layer present were classed as non-wetted.

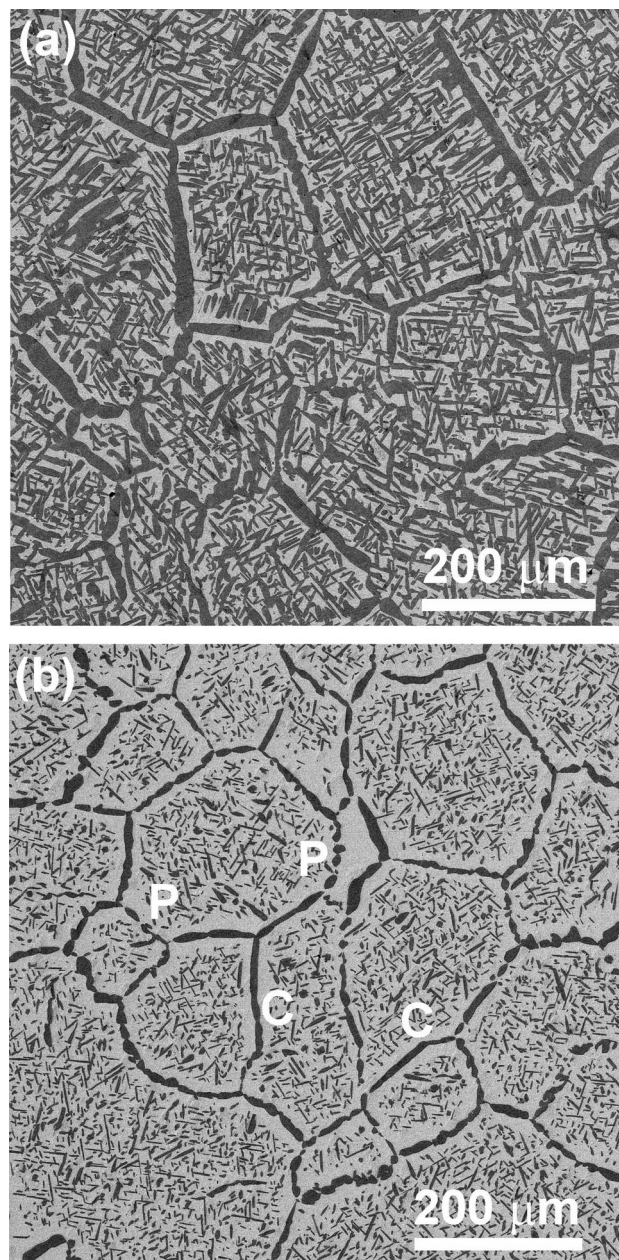
### 3. Results and Discussion

Figure 2 shows the typical examples of the observed microstructures. It contains SEM micrographs of the Ti-4.5 wt.% Fe and Ti-9 wt.% Fe alloys annealed at temperature 695°C during 1032 h. The  $\alpha(\text{Ti, Fe})$  phase appears dark. The  $\beta(\text{Ti, Fe})$  phase appears bright. The bright  $\beta(\text{Ti, Fe})$  phase contains 87.8 wt.% Ti and 12.2 wt.% Fe. The bright  $\beta(\text{Ti, Fe})$  phase mainly forms the bulk of the grains in the annealed polycrystal. The dark  $\alpha(\text{Ti, Fe})$  phase contains 99.9 wt.% Ti and 0.1 wt.% Fe. These values correspond to those in equilibrium phase diagram at 695 °C. The studied samples contain  $\beta(\text{Ti, Fe})/\beta(\text{Ti, Fe})$  grain boundaries completely (C) and partially (P) wetted by the second solid phase  $\alpha(\text{Ti, Fe})$ . The  $\beta(\text{Ti, Fe})/\beta(\text{Ti, Fe})$  grain boundaries completely wetted by the second solid phase  $\alpha(\text{Ti, Fe})$  contain the continuous layer of  $\alpha(\text{Ti, Fe})$  (marked in Fig. 2(b) by the letter C). In case of partially wetted  $\beta(\text{Ti, Fe})/\beta(\text{Ti, Fe})$  GBs, the layer of  $\alpha(\text{Ti, Fe})$  phase is not continuous and consists of a chain of lenticular  $\alpha(\text{Ti, Fe})$  particles (marked in Fig. 2(b) by the letter P).



**Fig. 1** The part of the bulk phase diagram Ti-Fe. Vertical thin lines show the studied concentrations, and dots show the annealing temperatures

Figure 3 presents the XRD patterns for the Ti-9 wt.% Fe alloy in the as-cast state and annealed at temperatures 595-815 °C. The as-cast alloy contains mainly  $\alpha(\text{Ti, Fe})$  with hexagonal closely packed (hcp) lattice. The Fe-rich body-centered cubic (bcc)  $\beta(\text{Ti, Fe})$  phase is almost absent. With increasing annealing temperature, the amount of  $\beta(\text{Ti, Fe})$  phase increases and the lattice period increases as well. It is because the increase in Fe concentration in the  $\beta(\text{Ti, Fe})$  phase leads to decrease in the lattice parameter (Ref 12-15). In turn, by changing annealing temperature, the iron concentration in  $\beta(\text{Ti, Fe})$  phase should follow the transus line in the Ti-Fe phase



**Fig. 2** SEM micrographs of the Ti-4.5 wt.% Fe (a) and Ti-9 wt.% Fe (b) alloys annealed at temperature 695°C, 1032 h. The  $\alpha(\text{Ti, Fe})$  phase appears dark. The  $\beta(\text{Ti, Fe})$  phase appears bright. Letter C marks the  $\beta(\text{Ti, Fe})/\beta(\text{Ti, Fe})$  GBs completely wetted by the second solid phase  $\alpha(\text{Ti, Fe})$ . Letter P marks the  $\beta(\text{Ti, Fe})/\beta(\text{Ti, Fe})$  GBs partially wetted by the  $\alpha(\text{Ti, Fe})$  phase



diagram (i.e., the border between  $(\alpha\text{Ti}) + (\beta\text{Ti, Fe})$  and  $(\beta\text{Ti, Fe})$  areas of the Ti-Fe equilibrium phase diagram, as shown in Fig. 1). Therefore, the iron concentration in  $\beta(\text{Ti, Fe})$  phase should decrease with increasing annealing temperature.

On a series of micrographs taken for each annealing temperature, we counted the portion of completely wetted  $\beta(\text{Ti, Fe})/\beta(\text{Ti, Fe})$  GBs. We considered GBs as completely wetted in the case when a layer of the second phase  $\alpha(\text{Ti, Fe})$  continuously passed from one GB triple junction to another. Figure 4 shows the temperature dependence of the portion of completely wetted  $\beta(\text{Ti, Fe})/\beta(\text{Ti, Fe})$  GBs for Ti-1 wt.% Fe, Ti-2.8 wt.% Fe, Ti-4.3 wt.% Fe, Ti-6.5 wt.% Fe and Ti-9 wt.% Fe alloys. Due to the very small amount of  $\alpha(\text{Ti, Fe})$  phase, it was not possible to find the completely wetted GBs in the Ti-1 wt.% Fe alloy. In other studied alloys (Ti-2.8 wt.% Fe, Ti-4.3 wt.% Fe, Ti-6.5 wt.% Fe and Ti-9 wt.% Fe), the portion of completely wetted GBs increases with increasing annealing temperature. Moreover, the portion of completely wetted GBs at each temperature increases with increasing Fe content. The reason for this effect is the increase in amount of wetting  $\alpha(\text{Ti, Fe})$  phase. For the first time, this effect of the so-called apparently complete GB wetting has been observed in the Cu-In alloys (Ref 16). The physical reason for the increase in portion of wetted GBs is the decrease in contact angles between GBs and wetting phase. However, according to the lever rule, the amount of wetting phase in the two-phase area of the phase diagram also increases as the temperature increases from 595 to 882 °C. If the amount of the wetting phase is large, its layers would separate the grains even if the contact angle  $\theta > 0^\circ$ . In any case, Fig. 4 shows that only few  $\beta(\text{Ti, Fe})/\beta(\text{Ti, Fe})$  GBs are completely wetted by a layer of the second phase  $\alpha(\text{Ti, Fe})$  slightly above the temperature of eutectoid transformation 595 °C. Second important fact is that even close to the transus temperature the portion of completely wetted  $\beta(\text{Ti, Fe})/\beta(\text{Ti, Fe})$  GBs does not exceed ~ 80%.

We can try to extrapolate the curves for Ti-2.8 wt.% Fe, Ti-4.3 wt.% Fe and Ti-6.5 wt.% Fe alloys in Fig. 4 up to 100% of completely wetted GBs. Such temperatures of 100% GB wetting lie above the transus line. For Ti-4.3 wt.% Fe and Ti-6.5 wt.% Fe alloys, we obtain the temperatures close to  $T_{100\%} = 790 \pm 10$  °C. For the Ti-2.8 wt.% Fe alloy, this tem-

perature is about  $T_{100\%} = 840 \pm 10$  °C. Figure 5 shows the temperature dependence of the thickness of  $\alpha(\text{Ti, Fe})$  phase in the  $\beta(\text{Ti, Fe})/\beta(\text{Ti, Fe})$  GBs layer for the Ti-1 wt.% Fe, Ti-2.8 wt.% Fe, Ti-4.3 wt.% Fe, Ti-6.5 wt.% Fe and Ti-9 wt.% Fe alloys. The grain boundary layer thickness increases with increasing temperature of annealing and is almost independent in the Fe concentration. The GB layer thickness increases with increasing annealing temperature because of fixed annealing duration (about 720 h) and increasing bulk diffusion coefficient  $D$  of iron in titanium. On the other hand,  $D$  decreases only quite weak with increasing iron content in titanium (Ref 17).

Thus, we observed that the morphology of  $\alpha(\text{Ti, Fe})$  phase in the  $\beta(\text{Ti, Fe})/\beta(\text{Ti, Fe})$  GBs in the Ti-Fe alloys strongly depends on the annealing temperature. In turn, the mechanical and other performance properties of titanium alloys are controlled by the structure and morphology of the constituent phases (Ref 3-6). In this work, we, therefore, observed that the morphology of the phases in titanium alloys can be determined not only by the

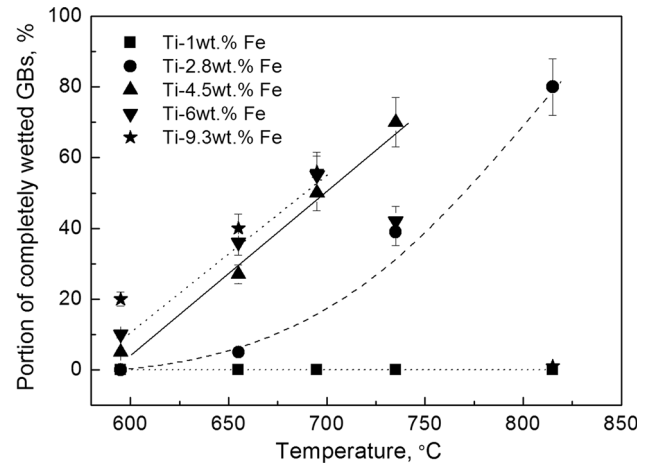


**Fig. 4** Temperature dependence of the portion of completely wetted  $\beta(\text{Ti, Fe})/\beta(\text{Ti, Fe})$  GBs for Ti-1 wt.% Fe, Ti-2.8 wt.% Fe, Ti-4.3 wt.% Fe, Ti-6.5 wt.% Fe and Ti-9 wt.% Fe alloys

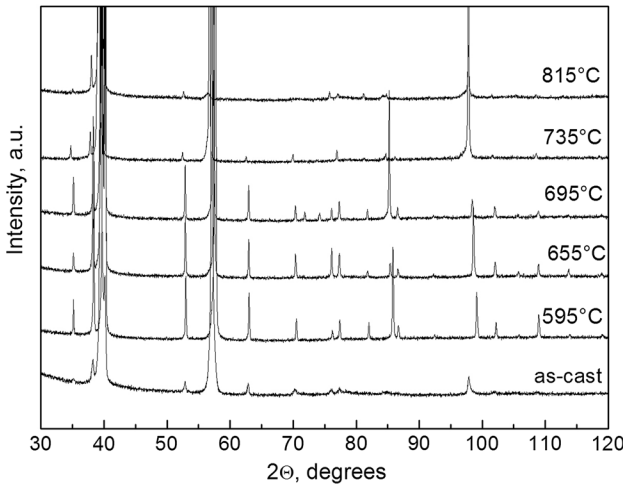


**Fig. 3** XRD patterns for the Ti-9 wt.% Fe alloy in the as-cast state and annealed at temperatures 595-815 °C

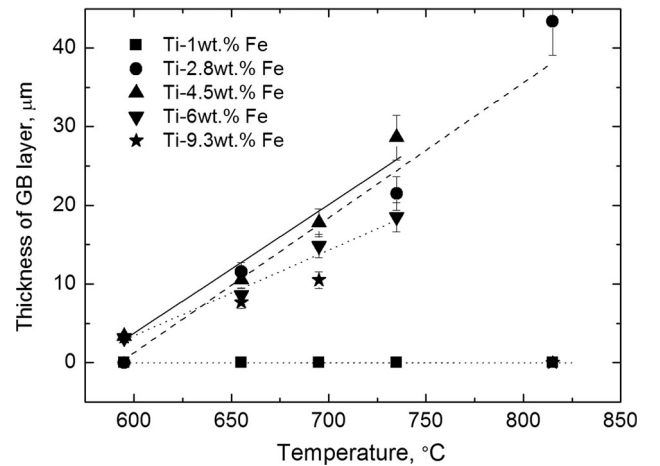


**Fig. 5** Temperature dependence of the thickness of layer of  $\alpha(\text{Ti, Fe})$  phase in the  $\beta(\text{Ti, Fe})/\beta(\text{Ti, Fe})$  GBs for Ti-1 wt.% Fe, Ti-2.8 wt.% Fe, Ti-4.3 wt.% Fe, Ti-6.5 wt.% Fe and Ti-9 wt.% Fe alloys

well-known bulk phase transitions, but also by the so-called grain boundary phase transitions like GB wetting/dewetting. It is well known that the so-called GB rims of  $\alpha(\text{Ti, Fe})$  phase in the  $\beta(\text{Ti, Fe})/\beta(\text{Ti, Fe})$  GBs are frequently observed in the Ti-based alloys (Ref 18–22). The presence of absence of such GB “rims” leads to the change of the mechanical properties of Ti alloys like cutting workability (Ref 19). The continuous GB “rims” of a second phase can also lead to the cracks formation during failure (Ref 21, 22). Thus, the GB phase transformations (like GB wetting/dewetting) can influence the properties of Ti alloys similarly to the influence of “conventional” bulk phase transformations.

## 4. Conclusions

The microstructure of Ti-Fe polycrystals in the  $\alpha + \beta$  two-phase area of the equilibrium phase diagram has been studied. The  $\alpha(\text{Ti, Fe})$  phase can form continuous or discontinuous layers in the  $\beta(\text{Ti, Fe})/\beta(\text{Ti, Fe})$  grain boundaries. Continuous layers correspond to the complete wetting of  $\beta(\text{Ti, Fe})/\beta(\text{Ti, Fe})$  GBs by a second solid phase  $\alpha(\text{Ti, Fe})$ . Discontinuous layers correspond to the incomplete (or partial) GB wetting by a second solid phase. The portion of completely wetted  $\beta(\text{Ti, Fe})/\beta(\text{Ti, Fe})$  GBs monotonously increases with increasing temperature. So does also the thickness of continuous GB layer of  $\alpha(\text{Ti, Fe})$  phase. The effect of apparently complete GB wetting has been observed.

## Acknowledgments

The work was performed under the partial financial support of Russian Foundation for Basic Research (Grants 16-53-12007, 16-03-00285 and 18-03-00067), German Science Foundation (Grants IV 98/5-1, HA 1344/32-1), Ministry of Education and Science of the Russian Federation in the framework of the Program to Increase the Competitiveness of NUST “MISIS,” and Karlsruhe Nano Micro Facility.

## References

1. R. Boyer, E.W. Collings, and G. Welsch, *Materials Properties Handbook: Titanium Alloys*, ASM International, Materials Park, 1994
2. T.B. Massalski, Ed., *Binary Alloy Phase Diagrams*, 2nd ed., ASM International, Materials Park, 1990
3. O.A. Kaibyshev and F.Z. Utjashev, *Superplasticity, Structure Refinement and Processing of Difficult Deformable Alloys*, Nauka, Moscow, 2002
4. O.A. Kaibyshev, *Superplasticity of Industrial Alloys*, Metallurgy, Moscow, 1984
5. M.J. Donachie, Jr., *Titanium: A Technical Guide*, 2nd ed., ASM International, Materials Park, 2000
6. B.B. Straumal, O.A. Kogtenkova, A.S. Gornakova, V.G. Sursaeva, and B. Baretzky, Review: Grain Boundary Faceting-Roughening Phenomena, *J. Mater. Sci.*, 2016, **51**, p 382–404
7. B.B. Straumal, A.A. Mazilkin, and B. Baretzky, Grain Boundary Complexions and Pseudopartial Wetting, *Curr. Opin. Solid State Mater. Sci.*, 2016, **20**, p 247–256
8. G.A. López, E.J. Mittemeijer, and B.B. Straumal, Grain Boundary Wetting by a Solid Phase; Microstructural Development in a Zn-5 wt% Al Alloy, *Acta. Mater.*, 2004, **52**, p 4537–4545
9. A.S. Gornakova, B.B. Straumal, A.L. Petelin, and A.B. Straumal, Solid-Phase Wetting at Grain Boundaries in the Zr-Nb System, *Bull. Russ. Acad. Sci. Phys.*, 2012, **76**, p 102–105
10. O.A. Kogtenkova, B.B. Straumal, S.G. Protasova, A.S. Gornakova, P. Zięba, and T. Czeppe, Effect of the Wetting of Grain Boundaries on the Formation of a Solid Solution in the Al-Zn System, *JETP Lett.*, 2012, **96**, p 380–384
11. B.B. Straumal, A.S. Gornakova, Y.O. Kucheev, B. Baretzky, and A.N. Nekrasov, Grain Boundary Wetting by a Second Solid Phase in the Zr-Nb Alloys, *J. Mater. Eng. Perform.*, 2012, **21**, p 721–724
12. R. Ray, B.C. Giessen, and N.J. Grant, The Constitution of Metastable Titanium-rich Ti-Fe Alloys: An Order-Disorder Transition, *Metall. Trans.*, 1972, **3**, p 627–629
13. B.W. Levinger, Lattice Parameter of Beta Titanium at Room Temperature, *Trans. Am. Inst. Min. Met. Eng.*, 1953, **197**, p 195–200
14. S.G. Fedotov, N.F. Kvasova, and M.I. Ermolova, Decomposition of the Metastable Solid Solution of Titanium with Iron, *Dokl. Akad. Nauk SSSR*, 1974, **216**(2), p 363–366
15. L.N. Guseva and L.K. Dolinskaya, Metastable Phases in Titanium Alloys with Group VIII, Elements Quenched from the  $\beta$ -Region, *Izv. Akad. Nauk SSSR Met.*, 1974, **6**, p 195–202
16. A.B. Straumal, B.S. Bokstein, A.L. Petelin, B.B. Straumal, B. Baretzky, A.O. Rodin, and A.N. Nekrasov, Apparently Complete Grain Boundary Wetting in Cu-In Alloys, *J. Mater. Sci.*, 2012, **47**, p 8336–8343
17. R.F. Peart, Effect of Pressure on the Diffusion of Fe in Ti and Ti + 10% Fe, *Phys. Stat. Sol.*, 1967, **20**, p 545–550
18. B.A. Kolachev and V.S. Lyasotskaya, Correlation Between Diagrams of Isothermal and Anisothermal Transformations and Phase Composition Diagram of Hardened Titanium Alloys, *Metal Sci. Heat Treat.*, 2003, **45**, p 119–126
19. Y.B. Egorova, A.A. Il'in, B.A. Kolachev, V.K. Nosov, and A.M. Mamonov, Effect of the Structure on the Cutability of Titanium Alloys, *Metal Sci. Heat Treat.*, 2003, **45**, p 134–139
20. B.A. Kolachev, M.G. Veitsman, and L.N. Gus'kova, Structure and Mechanical Properties of Annealed  $\alpha + \beta$  Titanium Alloys, *Metal Sci. Heat Treat.*, 1983, **25**, p 626–631
21. A.V. Fishgoit, V.M. Maistrov, and M.A. Rozanov, Interaction of Short Cracks with the Structure of Metals, *Sov. Mater. Sci.*, 1988, **24**, p 247–251
22. V.N. Bobovnikov, V.V. Luk'yanenko, and A.V. Fishgoit, Effect of Particles of the Insoluble Phase  $\text{Al}_3\text{FeNi}$  on the Kinetics of Fatigue Crack Propagation in Alloy AK4-1, *Metal Sci. Heat Treat.*, 1982, **24**, p 191–194